Front. Earth Sci. 2022, 16(3): 744–756
https://doi.org/10.1007/s11707-021-0928-3

RESEARCH ARTICLE

Identifying the spatio-temporal variability of human activity intensity and associated drivers: a case study on the Tibetan Plateau

Cai LIU[1,2,3], Haiyan ZHANG[4], Fuping GAN (✉)[2,3], Yunge LU[3], Hao WANG[3], Jiahong ZHANG[3], Xing JU[3]

1 College of Earth Sciences, Chengdu University of Technology, Chengdu 610059, China
2 Key Laboratory of Airborne Geophysics and Remote Sensing Geology (Ministry of Nature Resources), Beijing 100083, China
3 China Aero Geophysical Survey and Remote Sensing Center for Natural Resources, Beijing 100083, China
4 Institute of Geographical Sciences and Natural Resources Research, Chinese Academy of Sciences, Beijing 100101, China

Abstract Human activities have significantly degraded ecosystems and their associated services. By understanding the spatio-temporal variability and drivers of human activity intensity (HAI), we can better evaluate the interactions between human and terrestrial ecosystems, which is essential for land-use related decision making and eco-environmental construction. As the "third pole," the Tibetan Plateau (TP) plays a strong role in shaping the global environment, and acts as an important ecological security barrier for China. Based on land-use/cover change data, environmental geographic data, and socioeconomic data, we adopted a method for converting different land use/cover types into construction land equivalent to calculate the HAI value and applied the Getis–Ord *Gi** statistic to analyze the spatio-temporal dynamics associated with HAI since 1980 on the TP. Thereafter, we explored the forces driving the HAI changes using GeoDetector software and a correlation analysis. The main conclusions are as follows: It was observed that HAI increased slowly from 3.52% to 3.65% during the 1980–2020 period, with notable increases in the western part of the Qaidam Basin and Hehuang Valley. Spatially, HAI was associated with a significant agglomeration effect, which was mainly concentrated in the regions of the Yarlung Zangbo and Yellow–Huangshui rivers. Both natural and anthropogenic factors were identified as important driving forces behind the spatial changes in HAI, of which soil type, gross domestic product, and population density had the greatest influence. Meanwhile, the temporal changes in HAI were largely driven by economic development. This information provides crucial guidance for territory development planning and ecological-protection policy decisions.

Keywords Tibetan Plateau, human activity intensity, GeoDetector, spatio-temporal variability, driving factors

1 Introduction

For millennia, humans have dramatically transformed the form and processes of ecosystems locally, regionally, and globally to reap their benefits (Vitousek et al., 1997; Waters et al., 2016). More than three-quarters of the terrestrial biosphere has been altered by human activity over the course of history and through to the present day (Ellis and Ramankutty, 2008). Frequent and intensive human activity has caused multiple environmental impacts, such as climate change, land-use change, loss of biosphere integrity, and degradation of ecosystems (Rockström et al., 2009; Costanza et al., 2014; Song et al., 2018). A quantitative evaluation of this anthropogenic disturbance is critical if we are to analyze the impact of human activity on the regional ecological environment (Liu et al., 2018).

In previous research, human activity intensity (HAI) has been quantitatively evaluated based on the changing environmental pressure caused by human activity itself, such as multi-index superposition analysis based on weight (Magalhães et al., 2015; Han and Cui, 2016), human-footprint analysis (Sanderson et al., 2002; Venter et al., 2016; Li et al., 2018; Yi et al., 2020), degree of human modification (Theobald, 2013; Kennedy et al., 2019), and anthropogenic biomes (Ellis and Ramankutty, 2008; Ellis et al., 2010). Meanwhile, other studies have focused on the

Received January 8, 2021; accepted June 21, 2021

E-mail: fpgan@aliyun.com

changes in land use and landscape caused by human activity (Liu, 1992; Zhao et al., 2015a; Xu et al., 2016a; Xu and Xu, 2017). Among them, land use is the most direct and primary form of human activity affecting the surface ecosystem. Xu et al. (2016a) developed an algorithm model for HAI and established a method of converting different types of land-use/cover change (LUCC) into construction-land equivalents. This method can accurately and comprehensively reflect the degree of land use based on interpretation of remote-sensing data and is applicable to different spatially based research fields. This method can also avoid the problems associated with data collection caused by the remote location of the Tibetan Plateau (TP) and the consequent lack of information in contrast to the mid-east regions of China (Xu et al., 2016a; Liu et al., 2017; Li et al., 2018). For example, before 2000, 1 km grazing intensity data were unavailable (Li et al., 2018). Thus, unlike other researchers, we calculated the HAI characteristics for the entire TP based on the LUCC data during the period 1980–2020.

Known variously as the roof of the world, the third pole of the world, and the water tower of Asia (Xu et al., 2008), the TP significantly affects Earth's climate system (Immerzeel et al., 2010; Yao et al., 2012), and functions as a high-altitude plateau biodiversity conservation site thanks to its rich species diversity (Myers et al., 2000). With a fragile and complicated ecosystem, the TP is highly sensitive to human disturbance. Owing to the effects of human activity and climate change, the TP has developed many ecological problems (Yu et al., 2012), including grassland degradation (Cui and Graf, 2009; Yin et al., 2014), soil erosion (Yu et al., 2012), wetland shrinkage (Yu et al., 2012; Zhang et al., 2019), glacial retreat (Immerzeel et al., 2020) and desertification (Cui and Graf, 2009). Therefore, it is crucial to evaluate the spatio-temporal dynamics of HAI and to explore its mechanisms. Previous studies had mapped spatio-temporal characteristics of HAI by employing different categories of human pressures (Zhao et al., 2015b; Li et al., 2018; Sun et al., 2020), and explored its relationship with ecosystem (Li et al., 2018; Sun et al., 2020). Fan et al. (2015) reported that HAI exhibited negative effects on the ecological environment in Tibet during 1990–2000. Since 2000, the expanding scale of human activities has gradually and positively transformed the ecological environment. Sun et al. (2020) proposed that change in human activity intensity, especially the implementations of ecological protection projects, may dominantly explain why the ecological quality in various counties of the TP improved between 2000 and 2015. However, Li et al. (2018) showed that the mean HAI increased 28.43% during 1990–2010, further threatening the ecosystem services on the TP and possibly necessitating more effective measures.

The previous studies on the TP have various limitations and deficiencies. First, most of these studies investigated the impact of HAI on ecological environment, without clarifying the driving forces behind HAI changes (Cui and Graf, 2009; Yin et al., 2014; Fan et al., 2015; Zhao et al., 2015a, 2015b; Jiang et al., 2016; Li et al., 2018; Zhang et al., 2019; Sun et al., 2020). Second, they were performed with county-scale or 1 km-scale data, which may have weakened the reliability of their results. To mitigate these deficiencies, the present study attempts the following objectives: (i) map the spatial changes in HAI on the TP between 1980 and 2020 based on 100 m scale LUCC data, and (ii) investigate the drivers behind HAI in terms of natural and anthropogenic causes using GeoDetector software and a correlation analysis. Understanding the spatio-temporal patterns and drivers of HAI contributes to our understanding of the effect of HAI on ecosystem services (Sun et al., 2020), biodiversity conservation (Venter et al., 2016), and the effectiveness of ecological protection projects (Tapia-Armijos et al., 2017), such as the Grain to Green Program, Returning Rangeland to Grassland Program, and Natural Forest Conservation Programs.

2 Materials and methods

2.1 Study area

The TP is located in the southwestern region of China, and includes the Tibet Autonomous Region and Qinghai Province, as well as parts of Xinjiang, Gansu, Sichuan, and Yunnan regions (Fig. 1) (Dong et al., 2018). Altitudes in this region are mainly in the range 3000–7000 m, averaging above 4500 m. Geomorphologically, the TP can be divided into three main tectono-topographic units. The first one is a flat plateau with an average altitude of ~5000 m in the central area. The second is characterized by a series of orogenic belts at the margins of the plateau with an average altitude of 5500–6500 m, such as the Himalaya and the Longmen Shan. The sedimentary basins, as the third unit, are widely distributed in and around the TP (Wang et al., 2014).

Given the diverse topography, the climate is extremely complex and both temperature and precipitation decrease from the southeastern to northwestern parts of the plateau (Immerzeel et al., 2005). Across the region, the annual average temperature ranges from −5.6°C to 17.6°C, and the daily temperature difference ranges from 14°C to 17°C. The precipitation distribution is extremely uneven, with annual precipitation in the Motuo area (in the southeast) exceeding 4000 mm, but only 17.6 mm in the Lenghu area (in the northwest) (Li et al., 2016a). Under global climate warming, the rising rate of temperature on the TP reached 0.3°C–0.4°C per decade during 1960–2012 (Chen et al., 2015), far exceeding the global mean (Trenberth et al., 2007). Precipitation has increased at the northern TP but decreased at the southern TP (Chen et al., 2015). In general, the precipitation increased by 0.001 m/year during the 2002–2012 period (Yao et al., 2012).

The topographic setting, as well as the atmospheric conditions, determine the sequence of alpine meadows, steppes, and deserts from southeast to northwest (Pei et al., 2009). Alpine meadows and steppes dominate the undisturbed vegetation, with *Kobresia* sp. and *Stipa* sp. as the major vegetation types, respectively (Bosch et al., 2017). Human activity involves mainly animal husbandry and agriculture, tourism, industrial and mining development, and the construction of major ecological projects (Zhang et al., 2015). However, increasing anthropogenic activity, especially overgrazing, has accelerated grassland degradation and soil erosion (Cui and Graf, 2009). Livestock numbers on the grasslands of Tibet and Qinghai have exceeded their natural carrying capacity by 45% (by as much as 115%–153% in some areas) (Qian et al., 2007). Soil erosion, which is significant related to livestock numbers, increased by 75 times over the past 50 years (an increase rate of 18.68 $t \cdot ha^{-1} \cdot yr^{-1}$) (Li et al., 2019).

2.2 Quantification of HAI

We used HAI, defined as the degree of natural cover use, transformation, and the algorithm model for human activity intensity with the exploitation of land surface by humans in a certain region from an LUCC perspective (Xu et al., 2016a), to evaluate the spatial and temporal variability of HAI on the TP from 1980 to 2020.

$$\mathrm{HAI} = \frac{S_{\mathrm{CLE}}}{S} \times 100\%, \tag{1}$$

$$S_{\mathrm{CLE}} = \sum\nolimits_{i=1}^{n} (SL_i \times CI_i), \tag{2}$$

where, S_{CLE} is the area of construction land equivalent, S is the total land area, SL_i is the area of LUCC type i, CI_i is the conversion coefficient of type i for construction land equivalent, and n is the number of LUCC types. The construction land equivalent (CLE) compares the effects of different human activities on the land surface and is reflected in the LUCC types. Its conversion coefficient is calculated step-by-step using a two-level algorithm.

2.3 Spatial autocorrelation analysis

The hot-spot analysis calculates the Getis-Ord *Gi** statistic for each feature in a data set. This analysis was used to explore each feature within the context of neighboring features. To be a statistically significant hot spot, a feature must have a high value and should also be surrounded by other features with high values.

The Getis-Ord *Gi** statistics is calculated as follows (Ord and Getis, 1995)

$$G_i^* = \frac{\sum_{j=1}^{n} w_{ij}x_j - \overline{X}\sum_{j=1}^{n} w_{ij}}{S\sqrt{\frac{n\sum_{j=1}^{n} w_{ij}^2 - \left(\sum_{j=1}^{n} w_{ij}\right)^2}{n-1}}}, \tag{3}$$

where x_j is the attribute value for feature j; w_{ij} is the spatial weight between feature i and j and:

$$\overline{X} = \frac{1}{n}\sum_{j=1}^{n} x_j \quad S = \sqrt{\frac{\sum_{j=1}^{n} x_j^2}{n} - \overline{X}^2}. \tag{4}$$

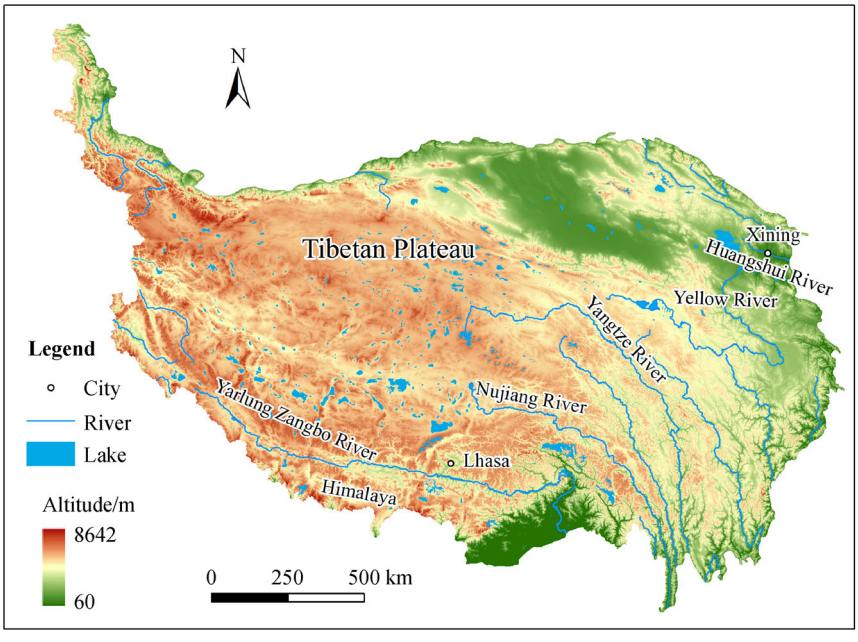

Fig. 1 Location of study area.

The Getis Ord *Gi** statistic is interpreted using standardised Z-scores. For statistically significant positive Z-scores, the larger the Z-score is, the more intense the clustering of high values (hot spot). For statistically significant negative Z-scores, the smaller the Z-score is, the more intense the clustering of low values (cold spot). From the statistical results, the hotspot pattern was divided into seven categories: very hot spot (confidence 99%), hot spot (confidence 95%), warm spot (confidence 90%), not statistically significant, cool spot (confidence 90%), cold spot (confidence 95%), and very cold spot (confidence 99%). Hotspot analysis was carried out through Arcgis10.2 software. We used ArcGIS' cluster-analysis tool (Getis-Ord *G**) to test for spatial autocorrelation in the occurrence of HAI hot spots in the study area.

2.4 GeoDetector

GeoDetector is a statistical tool used to measure stratified heterogeneity and reveal its causative factors (Wang et al., 2010). It is based on the following assumptions regarding the several subareas into which a study area has been divided. First, if the sum of the variance of the subareas is less than the regional total variance, spatially stratified heterogeneity exists. Second, if the spatial distribution of two variables tends to be consistent, there is a statistical correlation between them (Wang et al., 2016). GeoDetector contains four subdetectors: a factor detector, an interaction detector, a risk detector, and an ecological detector. Herein, we used the factor and interaction detectors to identify the key factors affecting the spatial distribution of HAI and to reveal whether any two factors had an interactive influence on HAI.

2.4.1 Factor detector

The factor detector explores the degree of stratified heterogeneity of HAI and measures the determinant power of each explanatory factor using the q-statistic (Wang et al., 2016). It is defined as follows:

$$q = 1 - \frac{\sum_{h=1}^{L} N_h \sigma_h^2}{N\sigma^2}, \tag{5}$$

where N and σ^2 are the number of units and the variance of HAI, respectively, and h represents the category of HAI or factor ($h = 1, 2, \ldots, L$). The q value ranges from 0 to 1 and indicates that the factor explains $100q\%$ of HAI, and the larger the q value is, the stronger the explanatory power of the factor to HAI.

2.4.2 Interaction detector

The interaction detector is used to analyze the effect of the interaction of two or more factors on HAI. Depends on the relationship between $q(X1 \cap X2)$ and $q(X1)$, $q(X2)$, the interaction of the two factor was divided into the following five categories:

Weaken, nonlinear: $q(X1 \cap X2) < \mathrm{Min}(q(X1), q(X2))$;

Weaken, uni-: $\mathrm{Min}(q(X1), q(X2)) < q(X1 \cap X2) < \mathrm{Max}(q(X1), q(X2))$;

Enhance, bi: $q(X1 \cap X2) > \mathrm{Max}(q(X1), q(X2))$;

Independent: $q(X1 \cap X2) = q(X1) + q(X2)$;

Enhance, nonlinear: $q(X1 \cap X2) > q(X1) + q(X2)$.

The $q(X1 \cap X2)$ stands for the explanatory power of the interaction of the two factors, $X1$ and $X2$, on HAI.

2.5 Data preparation and preprocessing

In our analysis, the HAI change and its driving forces were determined from multi-source data sets. The data types, spatial resolution, sources, and their related references can be found in Table 1. The LUCC data retrieved included 6 land-use categories (cropland, woodland, grassland, water-body, built-up land, and unused land) and 25 subclasses (Liu et al., 2014). Based on field surveys, the overall accuracy of the LUCC map was > 90% for the seven years listed in Table 1 (Zhang et al., 2012).

Changes to HAI are all linked in various ways to socioeconomic, environmental, and political factors (Turner et al., 1994; Fu et al., 2006; Liu et al., 2014; Yalew et al., 2016).We selected the HAI values from 2000 and 2015 as the dependent variables, and then selected nine natural and anthropogenic factors as the independent variables, namely, altitude, slope, soil type, precipitation, temperature, transportation system, economic development (gross domestic product (GDP)), population density, and nature reserves (Table 1). As the GeoDetector method is able to deal only with discrete variables (Wang et al., 2010), we converted the continuous variables into discrete variables using the geometrical interval method built into ArcGIS 10.2, which works reasonably well on data that are not distributed normally. The slope, altitude, precipitation, temperature, GDP, and population density were divided into 50 grades. Soil types were classified into 20 grades by soil order. Based on previous studies (Sanderson et al., 2002; Li et al., 2016b), we divided the distance to roads, expressways, and railways into six groups: 0–1, 1–3, 3–5, 5–7, 7–10, and 10–15 km.

3 Results

3.1 Spatio-temporal variation in HAI on the land surface

On the TP, HAI was between 3.52% and 3.65% over the period 1980–2020 (Fig. 2), which was lower than the national average (7.63% in 1984 and 8.54% in 2008) (Xu et al., 2016a). The spatial distribution of HAI is shown in Fig. 3. The middle and upper reaches of the Yarlung

Table 1 Data sets used in the present study

Data set	Data declaration	Time	Data sources
Land-use/cover	Raster; 100 m	1980, 1990, 2000, 2010, 2015, 2018, 2020	Resource and Environment Data Cloud Platform (available at Resource and Environment Science and Data Center website)
DEM[a)]	Raster; 90 m	2000	Geospatial Data Cloud site, Computer Network Information Centre, Chinese Academy of Sciences (available at Geospatial Data Cloud website)
Slope	Raster; 90 m	2000	National Tibetan Plateau Data Centre (available at TPDC website)
Precipitation and Temperature	Raster; 1 km	2000, 2015	National Tibetan Plateau Data Centre (Ding, 2019) (available at TPDC website)
GDP[b)] and Population density	Raster; 1 km	2000, 2015	Resource and Environment Data Cloud Platform (available at Resource and Environment Science and Data Center website)
Soil type	Vector; 1:1,000,000	1995	Institute of soil science, Chinese Academy of Sciences
Transportation	Vector; 1:1,000,000	1995, 2018	Resource and Environment Data Cloud Platform (available at Resource and Environment Science and Data Center website)
Nature reserves	Vector; 1:1,000,000	2018	Resource and Environment Data Cloud Platform (available at Resource and Environment Science and Data Center website)

Notes: a) DEM: digital elevation model; b) GDP: gross domestic product.

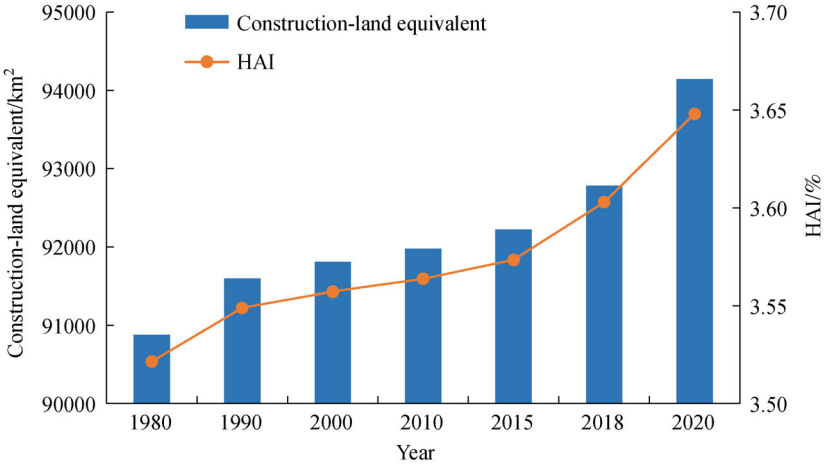

Fig. 2 Changes in the CLE area and HAI on the land surface on the TP between 1980 and 2020.

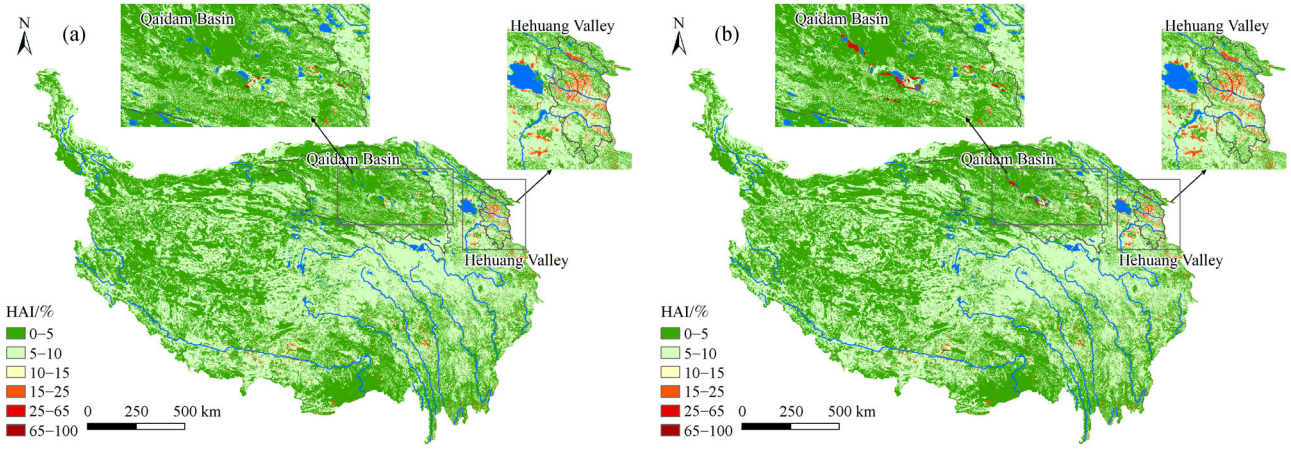

Fig. 3 Spatial distribution of HAI on the land surface on the TP in (a) 1980 and (b) 2020.

Zangbo River (3.95% to 4.08%) and the Yellow River–Huangshui River region (6.02% to 6.31%) exhibited high HAI, particularly in the Hehuang Valley (7.78% to 8.26%; Fig. 3), where more suitable natural conditions facilitated greater human activity. In other regions, HAI was extremely low, particularly on the southern slopes of the Himalaya (1.74% to 1.74%). Over the past 41 years, the average annual increase of HAI on the TP was 0.032 ‰, significantly below the national average (0.36 ‰) (Xu et al., 2016a). However, there were remarkable increases over this 41 year period in the western part of the Qaidam Basin (Fig. 3(b)), with the increase of 25.38%, and in the Hehuang Valley (Fig. 3(b)), with an increase of 6.17%.

3.2 Spatial autocorrelation analysis of HAI on the land surface

Getis-Ord *G** statistical analysis (pass *Z* test value, $P = 0$) showed that the clustering of HAI hot- and cold-spots on the TP during the study period was obvious. Between 1980 and 2020, hot and very hot regions increased from 2.49% to 2.89%, cold regions decreased from 12.94% to 9.11%, while some warm regions and cool regions tended to become statistically insignificant regions.

For 1980, the spatial distribution maps of HAI hotspots showed that hot regions were highly clustered and concentrated in the Yarlung Zangbo River and Yellow River–Huangshui River regions (Fig. 4(a)). The cold regions correspond mainly to desert areas, such as the southern part of the Xinjiang, northern part of the Qinghai and Tibet. Moreover, the southern slopes of the Himalaya were a cold region. Compared with 1980, the distribution of hot and cold regions by 2020 remained almost the same (Fig. 4(b)), with a new HAI hotspot area had appeared in the western part of the Qaidam Basin. Overall, the distribution of statistically significant hot regions was similar to that of built-up land, and the changes in hot regions between 1980 and 2020 were concentrated mainly in the Hehuang Valley and around the mining towns in the Qaidam Basin (Fig. 4(c)).

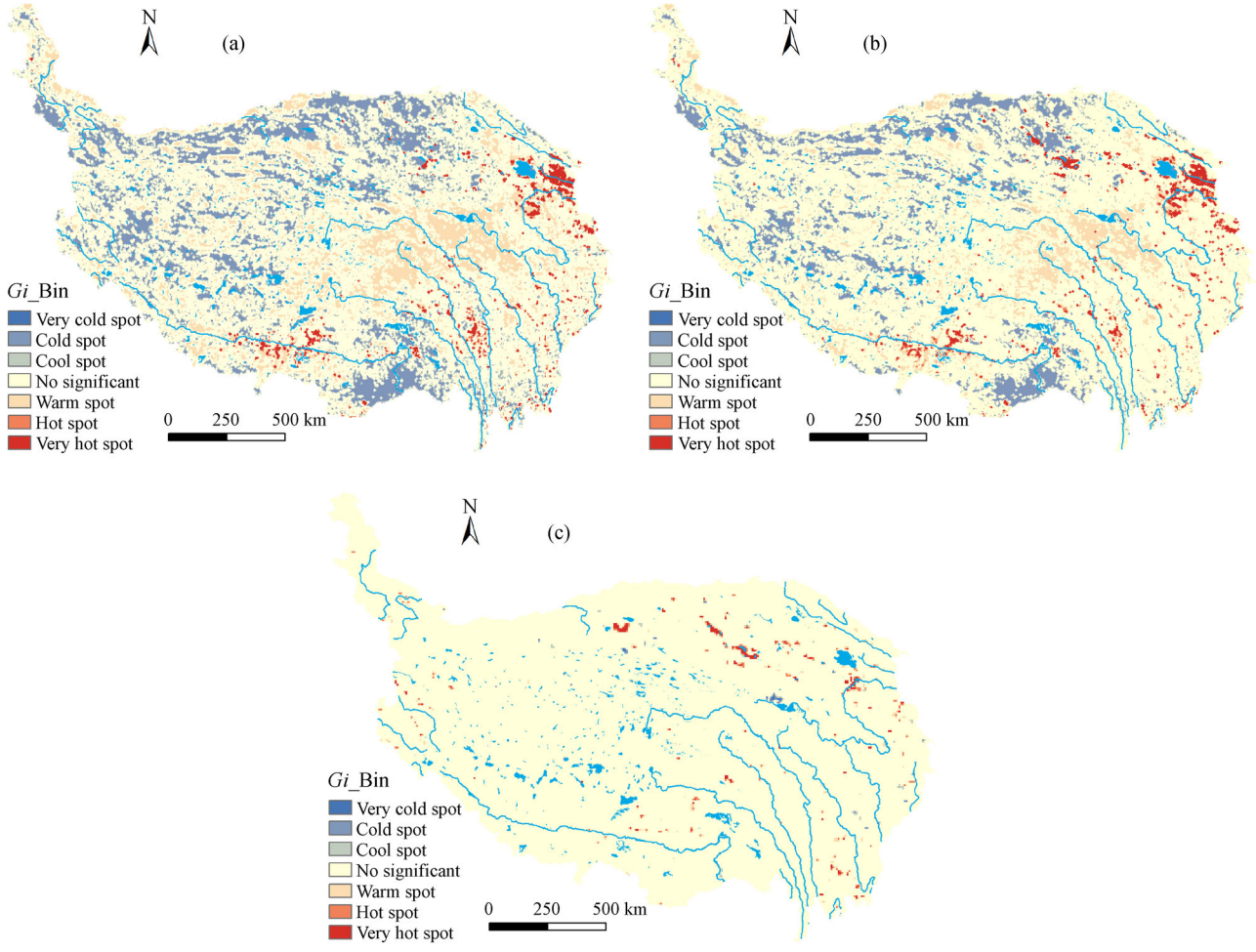

Fig. 4 Hotspot mapping of HAI on the land surface on the TP for (a) 1980, (b) 2020, and (c) 1980–2020.

3.3 Factors influencing spatial variability in HAI on the land surface

3.3.1 Influence of single factors on spatial variability in HAI on the land surface

According to the results of our factor detection analysis across the entire TP (Table 2), the major factors that influenced the spatial variability of HAI were soil type, GDP, and population density. In 2015, the factors related to GDP, soil type, population density, precipitation, and transportation systems explained 8.22%, 5.66%, 4.32%, 3.50%, and 2.23%, respectively. The contribution of temperature was the lowest (0.72%). Therefore, both natural and anthropogenic factors were identified as important factors that affected HAI change on the TP.

In Qinghai, soil type, GDP, and population density were the dominant factors in the spatial variability of HAI, followed by precipitation (Table 2). In contrast to Qinghai, the spatial variability of HAI in Tibet was dominated by precipitation (5.56%), soil type (5.17%), and GDP (3.81%) in 2000. However, the contribution of population density increased from 2.97% in 2000 to 5.93% in 2015, became another major factor. Moreover, both in Qinghai and Tibet, GDP became the most significant influencing factor, and the explanatory abilities of most environmental factors decreased in 2015.

Figure 5 shows the results of the Pearson correlation analysis between all continuous variables and HAI. The slope, GDP, population density, and transportation were highly significantly related to HAI, with Pearson correlation coefficients of $|r| > 0.8$ ($p < 0.05$), and altitude was also exhibited close relationships with HAI ($0.8 > |r| > 0.6$). Furthermore, the absolute value of the correlation coefficient between precipitation and HAI decreased in 2015 (Fig. 5(c)). Among these factors, GDP, population density, and transportation were positively correlated with HAI, and slope, altitude, and precipitation were negatively correlated.

Our results showed a highly significant correlation

Table 2 q value of single factors for the spatial variability in human activity intensity on the land surface

	Year	Slope	Altitude	Precipitation	Temperature	Soil type	GDP	Population density	Transportation
Tibetan Plateau	2000	0.017**	0.015**	0.035**	0.011**	0.065**	0.046**	0.054**	0.022**
	2015	0.014**	0.014**	0.035**	0.007**	0.057**	0.082**	0.043**	0.023**
Qinghai	2000	0.013**	0.045**	0.060**	0.047**	0.114**	0.105**	0.108**	0.045**
	2015	0.012**	0.040**	0.068**	0.031**	0.112**	0.130**	0.081**	0.036**
Tibet	2000	0.034**	0.035**	0.056**	0.018**	0.052**	0.038**	0.030**	0.010**
	2015	0.029**	0.031**	0.064**	0.016**	0.047**	0.082**	0.059	0.013**

Notes: '**': $p < 0.01$; '*': $p < 0.05$.

Table 3 q value for the interactions between factors for the spatial variability in human activity intensity on the land surface, Tibetan Plateau

	Year	Slope	Altitude	Precipitation	Temperature	Soil type	GDP	Population density	Transportation
Slope	2000	0.017**							
	2015	0.014**							
Altitude	2000	0.166**	0.015**						
	2015	0.163**	0.014**						
Precipitation	2000	0.118**	0.176**	0.035**					
	2015	0.120**	0.147**	0.035**					
Temperature	2000	0.107**	0.094**	0.125**	0.011**				
	2015	0.085**	0.077**	0.120**	0.007**				
Soil type	2000	0.105**	0.112**	0.137**	0.105**	0.065**			
	2015	0.102**	0.108**	0.129**	0.102**	0.057**			
GDP	2000	0.135**	0.081**	0.106**	0.085**	0.105*	0.046**		
	2015	0.211**	0.168**	0.217**	0.169**	0.203**	0.082**		
Population density	2000	0.180**	0.096**	0.171**	0.112**	0.123**	0.087*	0.054**	
	2015	0.073**	0.061**	0.082**	0.058**	0.093*	0.094*	0.043**	
Transportation	2000	0.128**	0.086**	0.124**	0.098**	0.116**	0.101**	0.128**	0.022**
	2015	0.120**	0.097**	0.137**	0.078**	0.117**	0.174**	0.071**	0.023**

Notes: '**': the nonlinear enhancement of two factors; '*': the bi-mutually enhancement of two factors Enhance.

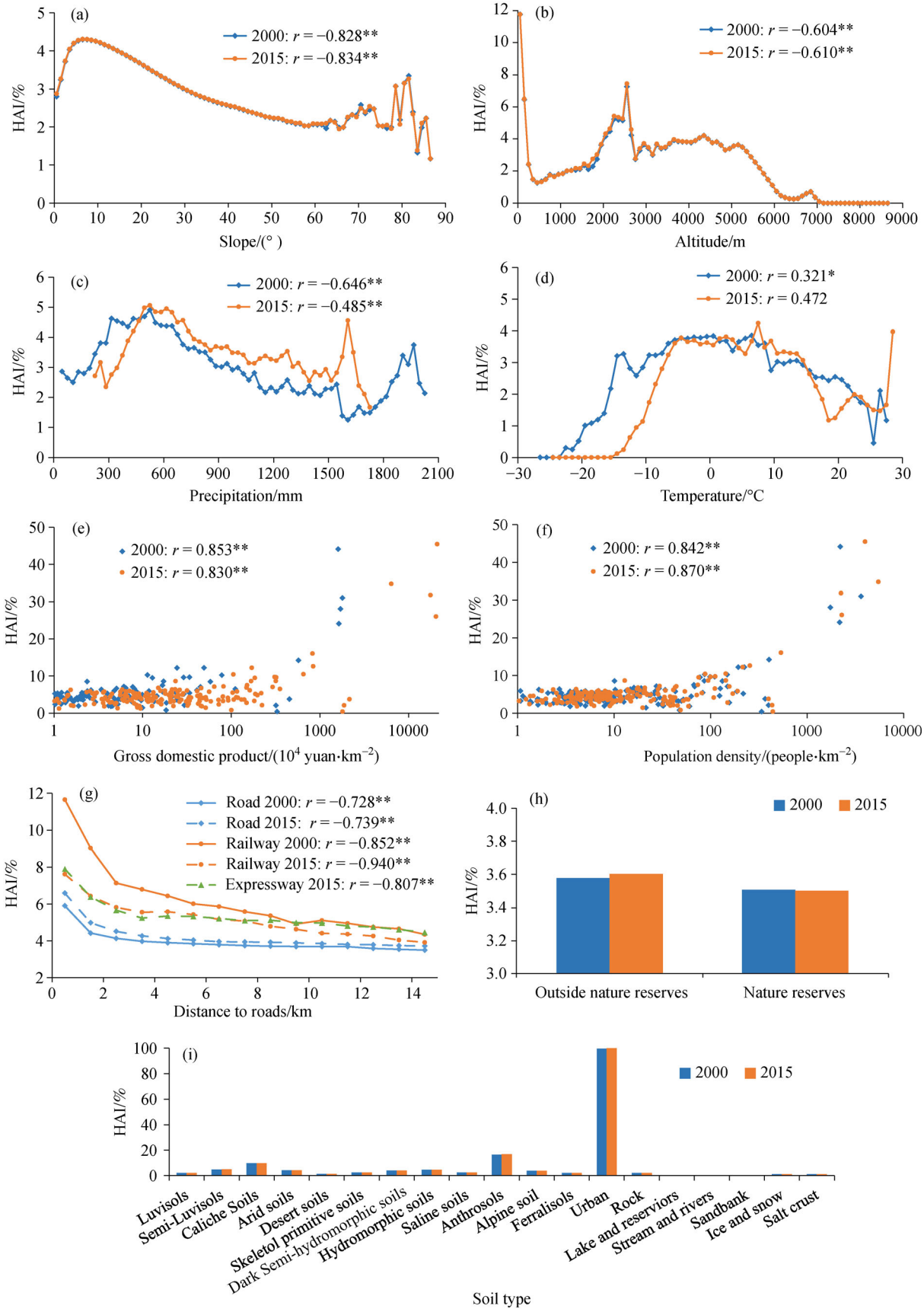

Fig. 5 Relationships on the TP in 2000 and 2015 between HAI on the land surface and (a) slope, (b) altitude, (c) precipitation, (d) temperature, (e) GDP, (f) population density, (g) distance to roads, (h) nature reserves, and (i) soil type. Notes: '**': $p < 0.01$; '*': $p < 0.05$.

between being within 15 km of a way and HAI. The HAI decreased with increasing distance especially within 3 km (Fig. 5(g)). Among all types of roads, expressways and railways exhibited greater and wider impact on HAI.

In addition, the TP has complex soil-diversity patterns. We calculated HAI for every soil type (Fig. 5(i)). The urban, anthrosols, and caliche soils exhibited high HAI (9.81% to 100%), whereas the ferralisols and desert soils exhibited low HAI (1.45% to 2.10%).

3.3.2 Influence of interactions between factors on spatial variability of HAI on the land surface

The results obtained, using interaction detection, showed that the influence of interactions between various factors were enhanced when compared with the influence of single factors, which indicated that the spatial variability of HAI was clearly affected by a series of interactions (Table 3). Across the entire region, the interactions of population density with slope, precipitation, and precipitation with altitude were the dominant factors affecting the HAI distribution in 2000. In 2015, the interactions of GDP with precipitation, slope, and soil type became the dominant factors.

4 Discussion

4.1 Key natural drivers of the spatial variability in HAI

Natural conditions (such as slope, altitude, climate, and soil type) are typically related to spatial changes in HAI (Fu et al., 2006; Yalew et al., 2016; Krajewski et al., 2018). We found that among the natural drivers, soil types exhibited the greatest effect on the spatial variability of HAI. Anthropogenic-alluvial soil and moisture soil, located in flat terrain with infiltration and recharge of groundwater and good hydrothermal conditions, which are important agricultural soil types in China (Hai and Chen, 2017), showed a high degree of HAI. In our study area, anthropogenic-alluvial soil and moisture soil distributed along the Yarlung Zangbo and Huangshui Rivers exhibited the highest HAI values, which were 22.41% and 20.65%, respectively, in 2015. Moreover, alpine soil, particularly frigid calcic, felty, frigid frozen, dark felty, and cold calcic soil, with a low degree of organic humus, weak mineral decomposition, and shallow soil, which were used mainly for seasonal grazing (Hai and Chen, 2017), are the main soil types found on the TP and cover more than 70.28% of the total area. Because of the low disturbance by human activity in the pastureland, the HAI of the alpine soil was approximately 3.79%.

In addition, slope and altitude also affected the spatial variability of HAI, which were consistent with the results of previous studies on the Loess Plateau (Fu et al., 2006). The HAI increased with a decrease in slope (Fig. 5(a)), indicating that people prefer to live in gently sloping, rather than steeply sloping areas. Moreover, steeper topographic features are not suitable for crop production and grazing due to accessibility challenges and environmental fragility. In particular, the highest HAI value in 2015 was 4.31% on slopes with gradients ranging from 6° to 7°.

The relationship between altitude and HAI was bimodal, with HAI peak values at 60–200 m and 2200–2600 m (Fig. 5(b)). One of these two peaks (where the altitude below 200 m) corresponded to grassland and cropland areas on the southern TP bordering India. The other main peak (where the altitude was 2200–2600 m) corresponded to an area mainly in the Hehuang Valley, which has a mild climate and a large population, and contains important agricultural production bases in Qinghai (Ding et al., 2014).

4.2 Key anthropogenic drivers of spatial variability in HAI

Anthropogenic factors also significantly affect the HAI. The rapidly growing population and increasing GDP directly affect the spatio-temporal variability of HAI (Turner et al., 1994; Sanderson et al., 2002; Venter et al., 2016; Krajewski et al., 2018; Hu et al., 2019). The results from GeoDetector and our correlation analysis indicated that GDP and population density played important roles in the spatial variability of HAI on the TP between 2000 and 2015. Economic development and human activity increased the associated demands on natural resources through expansion of cropland and grazing land, settlement areas, and other land uses (Zhang et al., 2019), which led to a higher HAI. In 2015, the population density was above 1000 people per km^2 (0.02% of the geographical area) in Lhasa and Xining, and the corresponding HAI was 37.26%. In the Hehuang Valley and the middle and upper reaches of the Yarlung Zangbo River, where the population density was between 50 and 1000 people per km^2 (1.11% of the geographical area), the HAI was 9.01%. In other areas, the population density was below 50 people per km^2, and the HAI was 3.51%.

In 2015, the spatial relationship between GDP and HAI followed a similar pattern to that between population density and HAI. In Lhasa and Xining, the GDP was above 10 million yuan per km^2 (0.03% of the geographical area), and the corresponding HAI was 27.91%. In Hehuang Valley, where the GDP was between 1.5 and 10 million yuan per km^2 (0.83% of the geographical area), the HAI was 9.00%, and in other areas, where the GDP was below 1.5 million yuan per km^2, the HAI was 3.52%.

Since the late 20th century, to mitigate increasing climate change, human activities and ecological and environmental challenges (such as glacial retreat, threatened biodiversity, grassland degradation, and natural disasters), the Chinese government has implemented several projects, including the Grain to Green Program

(Liu and Zheng, 2020), Returning Rangeland to Grassland Program, Natural Forest Conservation Programs (Ma et al., 2020), Protection and Construction Planning of Ecological Safety Shelter for Tibet (2008–2030), and Tibetan Plateau Environmental Construction and Protection Planning (2011–2030) (Sun et al., 2012).

After the implementation of Returning Rangeland to Grassland program on the TP began in 2004, the total numbers of livestock have decreased 7.8% (Xu et al., 2016b). During the 2004–2013 period, a total area of 6.4×10^4 km^2 of grasslands was fenced and artificial grasslands were established on 1.9×10^4 km^2 (Zhang et al., 2018). The alpine grassland gradually recovered through implementing multiple restoration measures (Xu et al., 2016b). In the "Three-River Headwaters" region (the Yangzte, Yellow, and Lantsang Rivers), as the implementation of projects, such as ecological conservation and restoration project in the Three-River Region, about 50000 local residents were removed from the reserve and relocated in nearby towns (Cai et al., 2015). Furthermore, the region's mean grassland yield was 30.31% higher during 2005–2015 period than in earlier periods, and the grazing pressure was significantly decreased (Zhang et al., 2014).

Moreover, 155 nature reserves have been created since 1963 on the TP, with a total area of ~82.2×10^4 km^2 (32.35% of the TP) (Zhang et al., 2015). Nature reserves are not suitable for analysis with GeoDetector, so we calculated the HAI inside and outside the reserves. In the present study, the mean HAI value within the nature reserves for 2000 was 3.507%, and it decreased to 3.500% in 2015 (Fig. 5(h)). Outside the nature reserves, the mean HAI increased from 3.576% in 2000 to 3.601% in 2015. The establishment of these nature reserves effectively limited HAI increase and played an important role in the effective protection of the fragile environment, which is consistent with the results of previous studies (Zhang et al., 2015; Zhu et al., 2019).

4.3 Key drivers of temporal variability in HAI

Our GeoDetector result revealed that the explanatory abilities of most natural environmental factors (such as soil type, slope, altitude, and temperature) decreased over the study period (Table 2), while the explanatory ability of GDP followed an obvious increase in Tibet and Qinghai. Between 2000 and 2015, we noted that while the GDP increased by 802.60% and the human population had grown 17.53%, the HAI increased by just 0.40% in Tibet and Qinghai. It appears that the economic development was increasing its efficiency in the use of land resources and simultaneously limiting the increase in HAI, which is in line with findings from other studies (Venter et al., 2016).

To investigate this, we analyzed the changes in industrial structure over the same period. By analyzing the statistical yearbook, we observed that the industrial structure of Tibet and Qinghai had changed considerably. In Tibet, with the change in industrial structure from single agriculture and animal husbandry to the scale of agriculture, industry, transportation, and service industries (Yang et al., 2015), the proportion of primary industries decreased by 21.50%, while those of the secondary and tertiary industries increased by 13.70% and 7.70%, respectively. The proportions contributed by tourism and construction to GDP also increased to 21.70% and 15.60%, respectively. In Qinghai, which has four pillar industries (i.e., petroleum, electric power, nonferrous metals, and the salt chemical industry), the contributions of the primary and tertiary industries to the GDP decreased by 6.60% and 2.10%, respectively, and that of the secondary industries increased by 9.20%. A previous study found that the contribution of the tertiary industries increased by 1.00%, and land-use efficiency increased by 0.104% (Chen et al., 2017).

In addition, high-tech application also improved land-use efficiency and GDP. Revenue from the principal business of the high-tech industries increased by 421.05% in Tibet, 4087.50% in Qinghai, and 1292.71% in China over the period 2000–2015. In addition, the total power of agricultural machinery increased by 530.62% in Tibet and 77.02% in Qinghai.

4.4 Comparisons with previous studies

Based on the LUCC data, we quantitatively evaluated the HAI effect on the TP. Overall, the HAI was low and increased slowly (by 3.69%) over the 1980–2020 period, consistent with previous studies (Zhao et al., 2015a, 2015b; Sun et al., 2020). Li et al. (2018) analyzed four categories of human pressures (LUCC, population density, road distribution, and grazing density), and found that HAI was generally low on the TP, but increased by 28.34% between 1990 and 2010, suggesting that the TP and its ecosystem services may face with more threats. However, cropland, night-time light, GDP, and power infrastructure also could measure the direct and indirect human pressures (Sanderson et al., 2002; Venter et al., 2016; Hu et al., 2019). Sun et al. (2020) selected eight categories of human impact factors (night-time light, GDP density, population density, distance to town, distance to road, ratio of cultivated land, grazing intensity, and the slope of NDVI) for HAI evaluation on the TP. They showed that the HAI increased by 3.98% from 2000 to 2015, consistent with our study.

In the present study, the drivers behind HAI changes were investigated from nine natural and anthropogenic factors: altitude, slope, soil type, precipitation, temperature, transportation system, economic development (GDP), population density, and nature reserves. The previous studies on HAI on the TP focused on the ecological environment rather than its driving mechanism. The natural driving forces have been especially neglected.

However, slope and altitude provided a crucial environmental context for population distribution in Tibet, and previous research had shown peak population densities at two altitudes (2600 m and 4000 m) (Liao and Sun, 2003). Among the research on anthropogenic factors, Li et al. (2018) assigned each of four anthropogenic factors a score ranging from 0 (least influential) to 10 (most influential), then summed the influence scores. To characterize the level of human disturbance on the TP, Zhao et al. (2015b) have assigned the same weight to three anthropogenic factors (population, number of villages, and road length). Both of these researches are likely to be insufficient. Sun et al. (2020) used the entropy weight method to calculate the weight of every anthropogenic factor, and hence evaluated the HAI. The population density carried the highest weight (0.20), followed by GDP (0.13), which is close and indicates the reliability of our method and results.

4.5 Uncertainty analysis and future perspectives

GeoDetector quantified the nonlinear responses of the independent variables and their influence on the spatial distribution of HAI. However, this method considers only the whole study area, not the local location. Geographical weighted regression (GWR) can assess the local relationship between comprehensive factors and HAI (Zhang et al., 2021). The combination of Geodetector and GWR may further improve the mapping accuracy. Also, owing to the large area and complex natural environment of the TP, we need to distinguish between the driving factors over different spatial scales. For example, we observed that population density exhibited the largest influence on the spatial variability of HAI in Lhasa City. In addition, we selected transportation system, GDP, population density, and nature reserves as indicators of human activities. Previous studies showed that grazing is another important indicator of human activities on the TP. Overgrazing is considered as the primary cause of grassland degradation and land desertification (Xu et al., 2016b). Further research should consider the addition of other impact factors such as livestock production.

5 Conclusions

With a fragile and complicated ecosystem, the TP is highly sensitive to human activities. Selecting the TP as a case study, this study quantitatively evaluated the spatio-temporal changes and drivers of HAI to reveal the major pattern of human activities, and to quantify the performance of ecological protection projects. The results will assist future science-based decision-making. The main conclusions are as follows. The HAI on the TP was low, and increased slowly from 3.52% in 1980 to 3.65% in 2020. Spatially, HAI was mainly concentrated in the regions of the Yarlung Zangbo and Yellow–Huangshui rivers. Both natural and anthropogenic factors had a significant influence on the spatial changes in HAI on the TP, and had an enhancement interaction effect between various factors. The soil type, GDP, and population density were the major contributory factors. Correlation analysis revealed that there were significant positive correlations between HAI and proximity to transportation, GDP, and population density, whereas slope, precipitation, altitude and nature reserves were negatively correlated with HAI. In addition, economic development was identified as an important driving force of temporal changes in HAI.

These results provide the foundation for the variety of stakeholders who are committed to the regional sustainable developments of economy and technology, particularly in supporting the adjustment of structure and distribution of land use and the utilization of land resources reasonably as well. However, what's important is that human beings, whether individuals, institutions, or governments, should moderate their influence in return for a more harmonious relationship with the natural world.

Acknowledgements This work was supported by the Key Laboratory of Airborne Geophysics and Remote Sensing Geology Foundation (No. 2020YFL20), China Postdoctoral Science Foundation (No. 2019M650820).

References

Bosch A, Schmidt K, He J S, Doerfer C, Scholten T (2017). Potential CO_2 emissions from defrosting permafrost soils of the Qinghai-Tibet Plateau under different scenarios of climate change in 2050 and 2070. Catena, 149: 221–231

Chen D L, Xu B Q, Yao T D, Guo Z T, Cui P, Chen F H, Zhang R H, Zhang X Z, Zhang Y L, Fan J, Hou Z Q, Zhang T H (2015). Assessment of past, present and future environmental changes on the Tibetan Plateau. Chin Sci Bull, 60(32): 3025–3035

Chen Z L, Li J K, Li J (2017). The influencing factors and spatial spillover effect of urban land use efficiency in China. Economic Survey, 34(4): 25–30 (in Chinese)

Cai H Y, Yang X H, Xu X L (2015). Human-induced grassland degradation/restoration in the central Tibetan Plateau: the effects of ecological protection and restoration projects. Ecol Eng, 83: 112–119

Cui X F, Graf H F (2009). Recent land cover changes on the Tibetan Plateau: a review. Clim Change, 94(1-2): 47–61

Costanza R, de Groot R, Sutton P, van der Ploeg S, Anderson S J, Kubiszewski I, Farber S, Turner R K (2014). Changes in the global value of ecosystem services. Glob Environ Change, 26: 152–158

Ding X H, Yu G X, Gao X C (2014). On the spatial pattern and coupling between the population and economy of Qinghai-Tibetan Plateau from 2000 to 2010. J Tibet U, 29(2): 34–42 (in Chinese)

Ding M J (2019). Temperature and precipitation grid data of the Qinghai-Tibet Plateau and its surrounding areas in 1998–2017 Grid data of annual temperature and annual precipitation on the Tibetan Plateau and its surrounding areas during 1998–2017. Beijing: National Tibetan Plateau Data Center

Dong M, Yan P, Liu B L, Wu W, Meng X N, Ji X R, Wang Y, Wang Y J

(2018). Distribution patterns and morphological classification of climbing dunes in the Qinghai-Tibet Plateau. Aeolian Res, 35: 58–68

Ellis E C, Ramankutty N (2008). Putting people in the map: anthropogenic biomes of the world. Front Ecol Environ, 6(8): 439–447

Ellis E C, Klein Goldewijk K, Siebert S, Lightman D, Ramankutty N (2010). Anthropogenic transformation of the biomes, 1700 to 2000. Glob Ecol Biogeogr, 19(5): 589–606

Fan J, Xu Y, Wang C S, Niu Y F, Chen D, Sun W (2015). The effects of human activities on the ecological environment of Tibet over the past half century. Chin Sci Bull, 60(32): 3057–3066

Fu B J, Zhang Q J, Chen L D, Zhao W W, Gulinck H, Liu G B, Yang Q K, Zhu Y G (2006). Temporal change in land use and its relationship to slope degree and soil type in a small catchment on the Loess Plateau of China. Catena, 65(1): 41–48

Hai C X, Chen J F (2017). Soil Geography. Beijing: Science Press

Han Z, Cui B S (2016). Development of an integrated stress index to determine multiple anthropogenic stresses on macrophyte biomass and richness in ponds. Ecol Eng, 90: 151–162

Hu M M, Li Z T, Wang Y F, Jiao M Y, Li M, Xia B C (2019). Spatio-temporal changes in ecosystem service value in response to land-use/cover changes in the Pearl River Delta. Resour Conserv Recycling, 149: 106–114

Immerzeel W W, Quiroz R, de Jong S (2005). Understanding precipitation patterns and land use interaction in Tibet using harmonic analysis of SPOT VGT-S10 NDVI time series. Int J Remote Sens, 26(11): 2281–2296

Immerzeel W W, van Beek L P H, Bierkens M F P (2010). Climate change will affect the Asian water towers. Science, 328(5984): 1382–1385

Immerzeel W W, Lutz A F, Andrade M, Bahl A, Biemans H, Bolch T, Hyde S, Brumby S, Davies B J, Elmore A C, Emmer A, Feng M, Fernández A, Haritashya U, Kargel J S, Koppes M, Kraaijenbrink P D A, Kulkarni A V, Mayewski P A, Nepal S, Pacheco P, Painter T H, Pellicciotti F, Rajaram H, Rupper S, Sinisalo A, Shrestha A B, Viviroli D, Wada Y, Xiao C, Yao T, Baillie J E M (2020). Importance and vulnerability of the world's water towers. Nature, 577(7790): 364–369

Jiang C, Li D Q, Wang D W, Zhang L B (2016). Quantification and assessment of changes in ecosystem service in the Three-River Headwaters Region, China as a result of climate variability and land cover. Ecol Indic, 66: 199–211

Kennedy C M, Oakleaf J R, Theobald D M, Baruch-Mordo S, Kiesecker J (2019). Managing the middle: a shift in conservation priorities based on the global human modification gradient. Glob Change Biol, 25(3): 811–826

Krajewski P, Solecka I, Mrozik K (2018). Forest landscape change and preliminary study on its driving forces in Ślęża Landscape Park (Southwestern Poland) in 1883–2013. Sustainability, 10(12): 4526

Li Q, Zhang C L, Shen Y P, Jia W R, Li J (2016a). Quantitative assessment of the relative roles of climate change and human activities in desertification processes on the Qinghai-Tibet Plateau based on net primary productivity. Catena, 147: 789–796

Li S C, Wang Z F, Zhang Y L, Wang Y K, Liu F G (2016b). Comparison of socioeconomic factors between surrounding and non-surrounding areas of the Qinghai-Tibet railway before and after its construction. Sustainability, 8(8): 776

Li S C, Zhang Y L, Wang Z F, Li L H (2018). Mapping human influence intensity in the Tibetan Plateau for conservation of ecological service functions. Ecosyst Serv, 30: 276–286

Li Y, Li J J, Are K S, Huang Z G, Yu H Q, Zhang Q W (2019). Livestock grazing significantly accelerates soil erosion more than climate change in Qinghai-Tibet Plateau: evidenced from ^{137}Cs and ^{210}Pbex measurements. Agric Ecosyst Environ, 285: 106643

Liao S B, Sun J L (2003). Quantitative analysis of relationship between population distribution and environmental factors in Qinghai-Tibet Plateau. China Population, Resources and Environment., 13(3): 62–67 (in Chinese)

Liu J Y (1992). Land Use in the Xizang (Tibet) Autonomous Region. Beijing: Science Press

Liu J Y, Kuang W H, Zhang Z X, Xu X L, Qin Y W, Ning J, Zhou W C, Zhang S W, Li R D, Yan C Z, Wu S, Shi X, Jiang N, Yu D, Pan X, Chi W (2014). Spatiotemporal characteristics, patterns, and causes of land-use changes in China since the late 1980s. J Geogr Sci, 24(2): 195–210

Liu H M, Gao J X, Zhang H Y, Ma X L, Xu X L (2017). Human disturbance monitoring and assessment in the biodiversity conservation priority area China. J Geo-inform Sci, 19(11): 1456–1465 (in Chinese)

Liu S L, Liu L M, Wu X, Hou X Y, Zhao S, Liu G H (2018). Quantitative evaluation of human activity intensity on the regional ecological impact studies. Acta Ecol Sin, 38(19): 6797–6809

Liu T, Zheng Y M (2020). Analysis of ecological compensation for returning farmland to forests in China. Issues Forest Economics, 40 (1): 21–28 (in Chinese)

Ma Z H, Xia C Q, Cao S X (2020). Cost-benefit analysis of China's Natural Forest Conservation Program. J Nat Conserv, 55: 125818

Magalhães J L L, Lopes M A, de Queiroz H L (2015). Development of a Flooded Forest Anthropization Index (FFAI) applied to Amazonian areas under pressure from different human activities. Ecol Indic, 48: 440–447

Myers N, Mittermeier R A, Mittermeier C G, da Fonseca G A B, Kent J (2000). Biodiversity hotspots for conservation priorities. Nature, 403 (6772): 853–858

Ord J K, Getis A (1995). Local spatial autocorrelation statistics: distribution issues and an application. Geogr Anal, 27(4): 286–306

Pei Z Y, Ouyang H, Zhou C P, Xu X L (2009). Carbon balance in an alpine steppe in the Qinghai-Tibet Plateau. J Integr Plant Biol, 51(5): 521–526

Qian S, Mao L X, Hou Y Y, Fu Y, Zhang H Z, Du J (2007). Livestock carrying capacity and balance between carrying capacity of grassland with added forage and actual livestock in the Qinghai-Tibet Plateau. Journal of Natural Resource,22: 389–397 (in Chinese)

Rockström J, Steffen W, Noone K, Persson A, Chapin F S 3rd, Lambin E F, Lenton T M, Scheffer M, Folke C, Schellnhuber H J, Nykvist B, de Wit C A, Hughes T, van der Leeuw S, Rodhe H, Sörlin S, Snyder P K, Costanza R, Svedin U, Falkenmark M, Karlberg L, Corell R W, Fabry V J, Hansen J, Walker B, Liverman D, Richardson K, Crutzen P, Foley J A (2009). A safe operating space for humanity. Nature, 461 (7263): 472–475

Sanderson E W, Jaiteh M, Levy M A, Redford K H, Wannebo A V, Woolmer G (2002). The human footprint and the last of the wild.

Bioscience, 52(10): 891–904

Song X P, Hansen M C, Stehman S V, Potapov P V, Tyukavina A, Vermote E F, Townshend J R (2018). Global land change from 1982 to 2016. Nature, 560(7720): 639–643

Sun H L, Zheng D, Yao T D, Zhang Y L (2012). Protection and construction of the national ecological security shelter zone on Tibetan Plateau. Acta Geogr Sin, 67(1): 3–12

Sun Y X, Liu S L,, Shi F N, An Y, Li M Q, Liu Y X (2020). Spatio-temporal variations and coupling of human activity intensity and ecosystem services based on the four-quadrant model on the Qinghai-Tibet Plateau. Sci Total Environ, 743: 140721

Tapia-Armijos M F, Homeier J, Draper Munt D (2017). Spatio-temporal analysis of the human footprint in South Ecuador: influence of human pressure on ecosystems and effectiveness of protected areas. Appl Geogr, 78: 22–32

Theobald D M (2013). A general model to quantify ecological integrity for landscape assessments and US application. Landsc Ecol, 28(10): 1859–1874

Trenberth K E, Jones P D, Ambenje P, Bojariu R, Easterling D, Klein Tank A, Parker D, Rahimzadeh F, Renwick J A, Rusticucci M, Soden B, Zhai P (2007). Observations: surface and atmospheric climate change. In: Solomon S, Qin D, Manning M, Chen Z, Marquis M, Averyt K B, Tignor M, Miller H L, eds. Climate Change 2007: The Physical Science Basis. Contribution of Working Group I to the Fourth Assessment Report of the Intergovernmental Panel on Climate Change. Cambridge: Cambridge University Press

Turner B L, Meyer W B, Skole D L (1994). Global land-use/land-cover change: towards an integrated study. Ambio, 23: 91–95

Venter O, Sanderson E W, Magrach A, Allan J R, Beher J, Jones K R, Possingham H P, Laurance W F, Wood P, Fekete B M, Levy M A, Watson J E (2016). Sixteen years of change in the global terrestrial human footprint and implications for biodiversity conservation. Nat Commun, 7(1): 12558

Vitousek P M, Mooney H A, Lubchenco J, Melillo J M (1997). Human domination of Earth's ecosystems. Science, 277(5325): 494–499

Wang C S, Dai J G, Zhao X X, Li Y L, Graham S A, He D F, Ran B, Meng J (2014). Outward-growth of the Tibetan Plateau during the Cenozoic: a review. Tectonophysics, 621: 1–43

Wang J F, Li X H, Christakos G, Liao Y L, Zhang T, Gu X, Zheng X Y (2010). Geographical detectors-based health risk assessment and its application in the neural tube defects study of the Heshun region, China. Int J Geogr Inf Sci, 24(1): 107–127

Wang J F, Zhang T L, Fu B J (2016). A measure of spatial stratified heterogeneity. Ecol Indic, 67: 250–256

Waters C N, Zalasiewicz J, Summerhayes C, Barnosky A D, Poirier C, Gałuszka A, Cearreta A, Edgeworth M, Ellis E C, Ellis M, Jeandel C, Leinfelder R, McNeill J R, Richter D, Steffen W, Syvitski J, Vidas D, Wagreich M, Williams M, Zhisheng A, Grinevald J, Odada E, Oreskes N, Wolfe A P (2016). The Anthropocene is functionally and stratigraphically distinct from the Holocene. Science, 351(6269): aad2622

Xu X D, Lu C G, Shi X H, Gao S T (2008). World water tower: an atmospheric perspective. Geophys Res Lett, 35(20): L20815

Xu Y, Xu X R, Tang Q (2016a). Human activity intensity of land surface: concept, method and application in China. J Geogr Sci, 26(9): 1349–1361

Xu H J, Wang X P, Zhang X X (2016b). Alpine grasslands response to climatic factors and anthropogenic activities on the Tibetan Plateau from 2000 to 2012. Ecol Eng, 92: 251–259

Xu X R, Xu Y (2017). Analysis of spatial-temporal variation of human activity intensity in Loess Plateau region. Geogr Res, 36(4): 661–672

Yalew S G, Mul M L, van Griensven A, Teferi E, Priess J, Schweitzer C, van Der Zaag P (2016). Land-use change modelling in the upper Blue Nile basin. Environments, 3(4): 21

Yang W F, Du L, Zhu G L (2015). Analysis of Tibetan industry development path based on the industrial evolution theory. Res Agri Modern, 36(5): 741–747 (in Chinese)

Yao T D, Thompson L G, Mosbrugger V, Zhang F, Ma Y M, Luo T X, Xu B Q, Yang X X, Joswiak D R, Wang W C, Joswiak M E, Devkota L P, Tayal S, Jilani R, Fayziev R (2012). Third pole environment (TPE). Environ Dev, 3: 52–64

Yi J, Du Y, Liang F, Tu W, Qi W, Ge Y (2020). Mapping human's digital footprints on the Tibetan Plateau from multi-source geospatial big data. Sci Total Environ, 711: 134540

Yin F, Deng X Z, Jin Q, Yuan Y W, Zhao C H (2014). The impacts of climate change and human activities on grassland productivity in Qinghai Province, China. Front Earth Sci, 8(1): 93–103

Yu C, Zhang Y, Claus H, Zeng R, Zhang X, Wang J (2012). Ecological and environmental issues faced by a developing Tibet. Environ Sci Technol, 46(4): 1979–1980

Zhang Z X, Zhao X L, Wang X, et al, eds. (2012). Land Use Remote Sensing Monitoring in China. Beijing: Star Map Press

Zhang L X, Fan J W, Shao Q Q, Tang P, Zhang H Y, Li Y Z (2014). Changes in grassland yield and grazing pressure in the Three River Headwater Region before and after the implementation of the eco-restoration project. Caoye Xuebao, 23: 116–123

Zhang Y L, Wu X, Qi W, Li S C, Bai W Q (2015). Characteristics and protection effectiveness of nature reserves on the Tibetan Plateau, China. Resource Sci, 37(7): 1455–1464 (in Chinese)

Zhang H Y, Fan J W, Wang J B, Cao W, Harris W (2018). Spatial and temporal variability of grassland yield and its response to climate change and anthropogenic activities on the Tibetan Plateau from 1988 to 2013. Ecol Indic, 95: 141–151

Zhang Y L, Liu L S, Wang Z F, Bai W Q, Ding M J, Wang X H, Yan J Z, Xu E Q, Wu X, Zhang B H, et al (2019). Spatial and temporal characteristics of land use and cover changes in the Tibetan Plateau. Chin Sci Bull, 64(27): 2865–2875 (in Chinese)

Zhang X, Yue Y, Tong X, Wang K, Qi X, Deng C, Brandt M (2021). Eco-engineering controls vegetation trends in southwest China karst. Sci Total Environ, 770: 145160

Zhao G S, Liu J Y, Kuang W H, Ouyang Z Y, Xie Z L (2015a). Disturbance impacts of land use change on biodiversity conservation priority areas across China:1990–2010. J Geogr Sci, 25(5): 515–529

Zhao H D, Liu S L, Dong S K, Su X K, Wang X X, Wu X Y, Wu L, Zhang X (2015b). Analysis of vegetation change associated with human disturbance using MODIS data on the rangelands of the Qinghai-Tibet Plateau. Rangeland J, 37(1): 77–87

Zhu P, Cao W, Huang L, Xiao T, Zhai J (2019). The Impacts of Human Activities on Ecosystems within China's Nature Reserves. Sustainability, 11(23): 6629